Hydroxyethylene Isostere Inhibitors of Human Immunodeficiency Virus-1 Protease: Structure–Activity Analysis Using Enzyme Kinetics, X-ray Crystallography, and Infected T-Cell Assays[†,‡]

Geoffrey B. Dreyer,[*,§] Dennis M. Lambert,[∥] Thomas D. Meek,[§] Thomas J. Carr,[§] Thaddeus A. Tomaszek, Jr.,[§] Annabellee V. Fernandez,[∥] Henry Bartus,[∥] Emilio Cacciavillani,[§] Anne M. Hassell,[⊥,#] Michael Minnich,[○] Stephen R. Petteway, Jr.,[∥] and Brian W. Metcalf[§]

Departments of Medicinal Chemistry, Antiinfectives, Macromolecular Sciences, and Protein Biochemistry, SmithKline Beecham Pharmaceuticals, P.O. Box 1539, King of Prussia, Pennsylvania 19406

Mitchell Lewis

The Johnson Research Foundation, Department of Biochemistry and Biophysics, School of Medicine, University of Pennsylvania, Philadelphia, Pennsylvania 19104

Received October 21, 1991; Revised Manuscript Received March 24, 1992

ABSTRACT: Analogues of peptides ranging in size from three to six amino acids and containing the hydroxyethylene dipeptide isosteres PheΨGly, PheΨAla, PheΨNorVal, PheΨLeu, and PheΨPhe, where Ψ denotes replacement of CONH by (*S*)-CH(OH)CH_2, were synthesized and studied as HIV-1 protease inhibitors. Inhibition constants (K_i) with purified HIV-1 protease depend strongly on the isostere in the order PheΨGly > PheΨAla > PheΨNorVal > PheΨLeu > PheΨPhe and decrease with increasing length of the peptide analogue, converging to a value of 0.4 nM. K_i values are progressively less dependent on inhibitor length as the size of the P1′ side chain within the isostere increases. The structures of HIV-1 protease complexed with the inhibitors Ala-Ala-X-Val-Val-OMe, where X is PheΨGly, PheΨAla, PheΨNorVal, and PheΨPhe, have been determined by X-ray crystallography (resolution 2.3–3.2 Å). The crystals exhibit symmetry consistent with space group $P6_1$ with strong noncrystallographic 2-fold symmetry, and the inhibitors all exhibit 2-fold disorder. The inhibitors bind in similar conformations, forming conserved hydrogen bonds with the enzyme. The PheΨGly inhibitor adopts an altered conformation that places its P3′ valine side chain partially in the hydrophobic S1′ pocket, thus suggesting an explanation for the greater dependence of the K_i value on inhibitor length in the PheΨGly series. From the kinetic and crystallographic data, a minimal inhibitor model for tight-binding inhibition is derived in which the enzyme subsites S2–S2′ are optimally occupied. The K_i values for several compounds are compared with their potencies as inhibitors of proteolytic processing in T-cell cultures chronically infected with HIV-1 (MIC values) and as inhibitors of acute infectivity (IC_{50} values). There is a rank-order correspondence, but a 20–1000-fold difference, between the values of K_i and those of MIC or IC_{50}. IC_{50} values can approach those of K_i but are highly dependent on the conditions of the acute infectivity assay and are influenced by physiochemical properties of the inhibitors such as solubility.

The aspartic protease of the human immunodeficiency virus-1 (HIV-1)[1] carries out the posttranslational processing of the viral *gag* and *gag–pol* proteins into functional viral components (Ratner et al., 1985; Kramer et al., 1986; Debouck et al., 1987; Petteway et al., 1991). The initial translation product of the *gag* gene, Pr55, is cleaved to yield the structural proteins of the virion core, namely, p17, p24, p7, and p6 (Veronese et al., 1987). Processing of the *gag–pol* translation product releases the viral replicative enzymes (protease, reverse transcriptase/ribonuclease H, and integrase). The protease is essential to the retroviral life cycle, since disrupting the proteolytic activity of HIV-1 through either site-directed mutagenesis (Kohl et al., 1988; Gottlinger et al., 1989; Peng et al., 1989) or addition of specific protease inhibitors (Meek et al., 1990; Roberts et al., 1990; Ashorn et al., 1990; Lambert et al., 1992) results in formation of noninfectious virions of aberrant morphology and prevents the spread of infection. These observations have led to extensive efforts to develop effective drugs targeting HIV-1 protease.

Analogues of peptide substrates in which the scissile dipeptide is replaced with mimetics of the proteolysis transition

[†] Supported in part by Grant GM-39526 from the National Institutes of Health. A preliminary account of this work was presented at the 22nd National Medicinal Chemistry Symposium, Austin, TX, July 30, 1990.

[‡] The crystallographic coordinates have been deposited in the Brookhaven Protein Data Bank under the file name 1aaq.

* Author to whom correspondence should be addressed.

[§] Department of Medicinal Chemistry, L420, SmithKline Beecham Pharmaceuticals.

[∥] Department of Antiinfectives, SmithKline Beecham Pharmaceuticals.

[⊥] Department of Macromolecular Sciences, SmithKline Beecham Pharmaceuticals.

Present address: Glaxo Inc., 5 Moore Drive, Research Triangle Park, NC 27709.

[○] Department of Protein Biochemistry, SmithKline Beecham Pharmaceuticals.

[1] Abbreviations: AIDS, acquired immunodeficiency syndrome; HIV-1, human immunodeficiency virus type 1; Boc, *tert*-butyloxycarbonyl; Cbz, benzyloxycarbonyl; HPLC, high-performance liquid chromatography; ^{1}H NMR, proton nuclear magnetic resonance; NOE, nuclear Overhauser effect; TBDMS, *tert*-butyldimethylsilyl; THF, tetrahydrofuran; IC_{50}, 50% inhibitory concentration by RT analysis; MIC, minimum inhibitory concentration by Western blot analysis; RT, reverse transcriptase; $TCID_{50}$, 50% infectious dose by viral titration in tissue culture; DMSO, dimethyl sulfoxide; EDTA, ethylenediaminetetraacetic acid; FBS, fetal bovine serum; Mes, 2-(*N*-morpholino)ethanesulfonic acid; PAGE, polyacrylamide gel electrophoresis; SDS, sodium dodecyl sulfate.

0006-2960/92/0431-6646$03.00/0

state are effective inhibitors of purified HIV-1 protease (Dreyer et al., 1989; Tomasselli et al., 1990; Rich et al., 1990; Roberts et al., 1990; Ashorn et al., 1990; Vacca et al., 1991; Lyle et al., 1991). In a direct comparison of several such transition-state mimetics, hydroxyethylene isosteres afforded particularly potent HIV-1 protease inhibitors in a purified enzyme assay (Dreyer et al., 1989). Some but not all of these inhibitors blocked viral replication in infected T-cell assays, suggesting that their antiviral activity depends not only on inhibition of the purified enzyme but also on molecular properties relating to their cell permeability and stability (Meek et al., 1990).

Realization of the antiviral potential of protease inhibitors will depend on the ability to proceed from initial lead structures to molecules which possess the spectrum of antiviral potency, low toxicity, and bioavailability required in a therapeutic agent. Low oral bioavailability and rapid biliary excretion of peptide-like inhibitors of human renin (also an aspartic protease) have impeded the development of such agents for hypertension (Humphrey & Ringrose, 1986; Greenlee, 1990). While factors affecting oral absorption and clearance mechanisms are poorly understood, efforts to overcome these problems include reduction of molecular weight and number of amide bonds and adjustment of lipophilicity. To provide a foundation for these efforts, in the present study we have used synthetic chemistry, enzymology, and X-ray crystallography to develop a detailed understanding of the relationships of inhibitor structure to enzyme inhibition. We have examined the effects of changes within a series of hydroxyethylene isosteres on their potency in the inhibition of purified HIV-1 protease, and from this we propose a minimum inhibitor structure necessary for tight-binding inhibition. We have also determined the three-dimensional structures of four complexes of HIV-1 protease with hydroxyethylene isostere inhibitors. The binding modes within these complexes help explain observed structure–activity relationships, point out the probable enzyme–inhibitor interactions involved in tight-binding inhibition, and suggest new inhibitor designs.

An essential component in guiding inhibitor modifications is the identification of relevant cell-based antiviral assays. A range of cell types is involved in HIV infection and AIDS pathogenesis (Fauci, 1988), each of which could respond differently to protease inhibitors. In this study, we have evaluated the antiviral activities of hydroxyethylene isosteres in two different infected cell systems and compared them with their enzyme inhibition constants. In one assay, within chronically infected T-cells, we have examined the ability of these compounds to inhibit processing of Pr55 into its functional components, thus interrupting the assembly of infectious virions. In a second, acute infection assay, we have examined their ability to inhibit infection of uninfected T-cells.

MATERIALS AND METHODS

Synthesis of Inhibitors

General. Tetrahydrofuran (THF) and toluene were distilled from sodium/benzophenone ketyl. Ether refers to commercial anhydrous diethyl ether. All other reagents and solvents were from commercial sources and were used without further purification. Flash chromatography was performed with E. Merck Kieselgel 60. Analytical and preparative HPLC were performed with Dynamax silica (5 μm) (Rainin). Proton nuclear magnetic resonance (^{1}H NMR) spectra were recorded at 250 MHz on a Bruker AM 250 spectrometer. Spectral and analytical data for all compounds are available as supplementary material.

(tert-Butyloxycarbonyl)phenylalanal (**2**). To a fine suspension of $LiAlH_4$ (0.912 g) in ether (80 mL) at −45 °C under Ar was added amide **1** (6.16 g) [prepared by the procedure of Goel et al. (1989): clear oil, $[\alpha]_{1365} = 31°$ (ethanol)] in ether (20 mL) with stirring. After 5 min the mixture was allowed to warm to 10 °C over 30 min and then was recooled to −45 °C, and a solution of 5.30 g of $KHSO_4$ in 15 mL of water was added cautiously. The cooling bath was removed and the thick mixture was stirred for 30 min. Ether (100 mL) and CH_2Cl_2 (100 mL) were added, the mixture was filtered through Celite, and the filter cake was rinsed with 100 mL each of ether and CH_2Cl_2. The filtrate was extracted with ice-cold 1 N HCl (3 × 50 mL), ice-cold 5% Na_2CO_3 (2 × 50 mL), and 100 mL of brine and then dried over $MgSO_4$, filtered, and concentrated by rotary evaporation at 30 °C to provide **2** (4.18 g, 84% yield) as a white solid: mp 82–83.5 °C; $[\alpha]_D = +35.3°$ (c = 1.00, CH_2Cl_2).

(5SR,6S)-7-Phenyl-6-[(tert-butyloxycarbonyl)amino]-5-hydroxyhept-1-ene (**3a,b**). 4-Bromo-1-butene (7.61 mL) was added over 25 min to a stirred suspension of Mg turnings (2.16 g) in ether (35 mL) under Ar, causing vigorous reflux. The mixture was heated to gentle reflux for an additional 20 min and then cooled to 0 °C (yield of Grignard reagent determined by titration: 65–70%). A solution of aldehyde **2** (5.26 g) in toluene (40 mL) was added over 10 min. After 1.5 h at 0 °C the clear reaction mixture was quenched cautiously with 3 N HCl. Extraction with ethyl acetate and concentration provided a yellow solid, which was dissolved in 50 mL of CH_3OH and stirred with $NaBH_4$ (200 mg) for 10 min. The mixture was diluted with 1 N HCl, extracted with CH_2Cl_2, and concentrated. Flash chromatography of the residue (gradient: 20%–40% ethyl acetate in hexanes) provided 5.03 g of **3a,b** as a white solid (78% yield). Analytical HPLC (15% ethyl acetate in hexanes) indicated a diastereomeric ratio (5*S*):(5*R*) of 7.20:1.00. Analytical samples of **3a** and **3b** were obtained by preparative HPLC. For **3a** (5*S*), mp 71–72 °C. Anal. C, H. N. For **3b** (5*R*), mp 148–149 °C. Anal. C, H, N.

(5S)-5-[(1'S)-1'-[(tert-Butyloxycarbonyl)amino]-2'-phenylethyl]tetrahydrofuran-2-one (**4a**). To a solution of alcohols **3a,b** (5.00 g; **3a**:**3b** = 7.2:1.0) in ethyl acetate (50 mL) were added triethylamine (4.56 mL), acetic anhydride (3.09 mL), and 4-(dimethylamino)pyridine (50 mg). After 3 h excess ethanol was added; the mixture was washed with 3 N HCl, 5% $NaHCO_4$, and water and then concentrated. The residue was stirred rapidly in 75 mL of 5:5:1 benzene/water/acetic acid with $(n\text{-Bu})_4NBr$ (160 mg) and $KMnO_4$ (7.9 g) for 2 h with intermittent cooling. The thick black mixture was cooled to 0 °C and 75 mL of saturated aqueous $NaHSO_3$ was added. After 15 min, the resulting white mixture was filtered through Celite, and the filtrate was extracted with ether. The ether extract was washed with water, dried ($MgSO_4$), filtered, and concentrated to a foam (6.9 g), which was then taken up in methanol (100 mL) and stirred at 60 °C with $NaOCH_3$ (ca. 10 g) for 18 h. The mixture was concentrated to ca. 25 mL, diluted with 10% HCl, and extracted with CH_2Cl_2. The organic layer was dried over $MgSO_4$, filtered, and stirred with *p*-toluenesulfonic acid (80 mg) and 3-Å molecular sieves (5 g) for 24 h. Filtration, concentration, and flash chromatography (gradient: 20%–30% ethyl acetate in hexanes) provided lactone **4a** (2.59 g, 52% yield), followed by lactone **4b**. For **4a**, mp 95–96 °C. Anal. C, H, N.

Alkylation of Lactone **4a** *(Illustrated for Compound* **5***).* *(3R,5S)-5-[(1'S)-1'-[(tert-Butyloxycarbonyl)amino]-2'-*

phenylethyl]-3-methyltetrahydrofuran-2-one (**5**). A solution of lactone **4a** (1.07 g, 3.50 mmol) in THF (3.0 mL) was added over 5 min to a solution of lithium diisopropylamide (monotetrahydrofuran) (7.70 mmol) in cyclohexane (5.1 mL) and THF (5.0 mL) under Ar at −78 °C. After 20 min, hexamethylphosphoric triamide (7.0 mmol) was added, followed by methyl iodide (7.0 mmol). After an additional 45 min at −78 °C, the mixture was diluted with 1 N HCl and extracted with CH_2Cl_2. The organic layer was concentrated, and the residue was purified by flash chromatography (30% ethyl acetate in hexanes) and then by HPLC (20% ethyl acetate in hexanes) to provide lactone **5** (883 mg, 79% yield): mp 134.5–135.0 °C. Anal. C, H, N.

Lactones **6**, **7**, and **10** were prepared by procedures similar to that described for lactone **5**, using allyl bromide, methallyl bromide, or benzyl bromide as the alkylating agent (yields: 70%, 72%, and 77%, respectively).

Lactones **8** and **9** were prepared in quantitative yield by catalytic hydrogenation of lactones **6** and **7** (1 atm of H_2, 10% Pd/C, ethyl acetate).

Preparation of Silyl-Protected Isosteres (Illustrated for Compound **12**). *(2R,4S,5S)-2-Methyl-4-(tert-butyldimethylsiloxy)-5-[(tert-butyloxycarbonyl)amino]-6-phenylhexanoic Acid* (**12**). The procedure of Evans et al. (1985) was used, beginning with 830 mg of lactone **5**. The crude product was purified by flash chromatography (gradient: 2%–4% methanol in $CHCl_3$) to provide 0.10 g of lactone **5** (12% yield) followed by 1.02 g of compound **12** (87% yield): mp 152–154 °C. Anal. C, H, N. The ^1H NMR spectrum of compound **12** displays evidence of conformational isomerism (approximate 2:5 ratio of two conformers), a phenomenon also observed with other silyl-protected isosteres.

Synthesis of Peptide Analogues (Illustrated for Compound IVb). *(2R,4S,5S)-[[2-Methyl-4-(tert-butyldimethylsiloxy)-5-[(tert-butyloxycarbonyl)amino]-6-phenylhexanoyl]valyl]-valine Methyl Ester* (**16**). Isobutyl chloroformate (34 μL, 0.26 mmol) was added dropwise to a stirring solution of 4-siloxy acid **12** (112 mg, 0.250 mmol) and *N*-methylmorphine (33 μL, 0.30 mmol) in THF (1.5 mL) under Ar at −40 °C. After 15 min, more *N*-methylmorpholine (50 μL, 0.45 mmol) was added, followed by a solution of valylvaline methyl ester hydrochloride (100 mg, 0.375 mmol) in THF (1.0 mL). The mixture was allowed to warm to room temperature and after 12 h was diluted with 5% HCl, extracted with ethyl acetate, concentrated, and purified by flash chromatography (25:1 $CHCl_3$/methanol) to provide **16** (154 mg, 93% yield) as a white solid.

(2R,4S,5S)-[[2-Methyl-4-(tert-butyldimethylsiloxy)-5-[[(benzyloxycarbonyl)alanyl]amino]-6-phenylhexanoyl]valyl]valine Methyl Ester (**18**). Compound **16** (154 mg, 0.233 mmol) was dissolved in trifluoroacetic acid (1 mL). After 5 min the solution was diluted with 5% Na_2CO_3 and extracted three times with CH_2Cl_2. The combined organic layers were washed with water and concentrated to provide **17** (124 mg, 95%). Isobutyl chloroformate (25 μL, 0.19 mmol) was added to a solution of Cbz-Ala (42.4 mg, 0.190 mmol) and *N*-methylmorpholine (25 μL, 0.23 mmol) in THF (1.0 mL) under Ar at −40 °C. After 3 min a solution of amine **17** (97 mg, 0.173 mmol) in THF (1.5 mL) was added. The cold bath was removed, and after 5 h the mixture was diluted with 5% HCl, extracted with $CHCl_3$, and concentrated. Flash chromatography (25:1 $CHCl_3$/methanol) provided compound **18** (99 mg, 75% yield) as a white foam.

(2R,4S,5S)-[[2-Methyl-4-(tert-butyldimethylsiloxy)-5-[[[(benzyloxycarbonyl)alanyl]alanyl]amino]-6-phenylhexanoyl]valyl]valine Methyl Ester (**19**). Compound **18** (99 mg, 0.129 mmol) was stirred in 3 mL of methanol with 30 mg of 10% Pd on carbon under hydrogen (1 atm) for 2.5 h. Filtration and concentration provided the unblocked peptide **19a** (75.3 mg, 92% yield). Isobutyl chloroformate (16.9 μL, 0.13 mmol) was added to a −40 °C solution of Cbz-Ala (29 mg, 0.13 mmol) and *N*-methylmorpholine (16.5 μL, 0.15 mmol) in THF (0.8 mL) under Ar with stirring. After 5 min compound **19a** (75.3 mg) was added as a solution in THF (1.0 mL). The cold bath was removed, and after 4 h extractive workup followed by flash chromatography (50:1 methanol/$CHCl_3$) provided compound **19** (93.3 mg, 94% yield). The ^1H NMR spectrum of this compound reveals conformation isomerism.

(2R,4S,5S)-[[2-Methyl-4-hydroxy-5-[[[(benzyloxycarbonyl)alanyl]alanyl]amino]-6-phenylhexanoyl]valyl]valine Methyl Ester (IVb). Compound **19** (93.3 mg) was dissolved in trifluoroacetic acid (1 mL). After 10 min the solution was diluted with $CHCl_3$ and shaken with 5% NaOH. The resulting emulsion was extracted with 90:10:1 $CHCl_3$/methanol/water, and then the organic layers were washed with water and concentrated. The residue was slurried in CH_2Cl_2 and filtered through a Celite plug, after which the clean product was eluted with 80:20:2 $CHCl_3$/methanol/water. Concentration of the eluant provided compound IVb (60 mg, 74% yield) as a white solid: mp 238–240 °C. Anal. C, H, N.

Enzymology

Source of Enzyme. Recombinant HIV-1 protease (Debouck et al., 1987) was purified to apparent homogeneity from bacterial cell lysates as described by Grant et al. (1991) and its protein content determined chromatographically as described by Strickler et al. (1989). The purified protease was routinely stored in 50 mM sodium acetate (pH 5.0), 0.35 M NaCl, 1 mM EDTA, 1 mM dithiothreitol, and 40% glycerol at −80 °C.

Enzyme Inhibition Studies. Protease inhibition was determined with the substrate Ac-Arg-Ala-Ser-Gln-Asn-Tyr-Pro-Val-Val-NH_2 (K_m = 5.5 mM, k_{cat} = 29 s^{-1}) as described (Moore et al., 1989; Dreyer et al., 1989). Inhibitors were dissolved in DMSO and diluted into reaction mixtures to a final DMSO content of 10%. For inhibitors with inhibition constants (K_i) greater than 40 nM, assay mixtures contained the substrate (1 mM), inhibitor (10–500 nM or 1–50 μM), and 10% DMSO in 50 μL of 50 mM Mes (pH 6.0), 1 mM EDTA, 200 mM NaCl, 1 mM dithiothreitol, and 0.1% Triton X-100 (MENDT buffer). Reaction was initiated by addition of purified protease (30 nM). Reaction mixtures were incubated at 37 °C for 20 min, then quenched with 1% trifluoroacetic acid (50 μL), and analyzed by reversed-phase HPLC. Inhibition constants were obtained by the method of Dixon (1953) assuming competitive inhibition.

For more potent inhibitors (K_i < 40 nM), the substrate (1 mM) was preincubated at 37 °C with inhibitor (0–100 nM) in 50 μL of MENDT buffer (pH 6.0) containing 10% DMSO. Reaction was initiated by addition of protease (1–40 nM). Reactions were quenched after 60 min (<15% reaction), and initial rates were determined as described above. The fractional inhibited velocities (v_i/v_0) were plotted versus inhibitor concentration at each enzyme concentration, and the data were fitted to eq 1 [v_i, inhibited velocity; v_0, uninhibited velocity; A, fraction of active enzyme; E, total enzyme concentration determined by protein assay; I, total inhibitor

$$v_i/v_0 = (AE - I - K + [(K + AE - I)^2 + 4KI]^{1/2})(2AE)^{-1} \quad (1)$$

Table I: Crystallographic Data for Inhibitor Complexes

inhibitor	no. of reflect.[a]	unique reflect.[b]	R-sym[c]	rms error (Å)[d]	R-factor[e] (%)	no. of crystals[f]	resolution (Å)[g]
Va	16 472	4302	4.3	(a) 0.02 (b) 0.04 (c) 0.04	18.3	3	2.3
Vb	11 376	3867	4.8	(a) 0.01 (b) 0.05 (c) 0.06	16.4	2	2.5
Vc	6 972	2111	5.3	(a) 0.02 (b) 0.08 (c) 0.03	16.6	2	3.2
Ve	12 467	3409	5.1	(a) 0.02 (b) 0.04 (c) 0.05	17.2	4	2.8

[a] Number of reflections measured. [b] Number of unique measurements in space group $P6_1$. [c] Symmetry R-value for equivalent reflections assuming space group symmetry $P6_1$. [d] rms deviation from ideal distances for (a) bond lengths, (b) angle distances, and (c) planar 1,4 distances. [e] Overall R-factor for the data. [f] Number of crystals used in data collection. [g] Effective resolution of the data.

concentration; $K = K_i(1 + S/K_m)$, where K_i is the inhibition constant, S is the substrate concentration, and K_m is the Michaelis constant of the substrate] (Williams & Morrison, 1979).

Time-dependent inhibition of HIV-1 protease was investigated by preincubation of inhibitors (0–500 nM) with protease (270 nM) at 37 °C for 0–120 min in 50 μL of MENDT buffer containing 10% DMSO. Aliquots (5 μL) were removed at intervals and diluted 10-fold into assay mixtures containing 3 mM substrate, and the fraction of remaining enzymatic activity (v_i/v_0) was determined at each interval as described above. Time-dependent inhibition was evaluated from plots of v_i/v_0 vs time.

Crystallography

Crystallization and Data Collection. Cocrystals of HIV-1 protease complexed with hydroxyethylene isostere analogues of Phe-Gly, Phe-Ala, Phe-NorVal, and Phe-Phe (compounds Va–c,e) were prepared by mixing the inhibitors with HIV-1 protease (5 mg/mL) at a molar ratio of 5:1 or 10:1. Crystals were grown by combining equivolume amounts of the precipitating solution, containing sodium acetate buffer (pH 5.0–5.6) and 0.2–0.8 M ammonium sulfate, and the solution of the protein–inhibitor complex. By use of the hanging drop vapor diffusion method, the enzyme–inhibitor complex was mixed with the precipitating solution on a siliconized cover glass, inverted, and sealed with silicone vacuum grease (Dow-Corning) over a reservoir containing 1 mL of the precipitating solution. Trays were incubated at 22 °C, and hexagonal-shaped rods appeared after 4–10 days. The space group and cell dimensions of all the crystals were screened by precession photography. All four protease–inhibitor complexes crystallized with symmetry consistent with either space group $P6_1$ having noncrystallographic 22 symmetry or space group $P6_122$. The unit cell dimensions were $a = b = 63.4$ Å and $c = 84.0$ Å.

The cocrystals were prepared for data collection using standard techniques. Three-dimensional diffraction data were recorded to a nominal resolution of 2.3 Å using a Siemens multiwire X-ray area detector. A rotating anode X-ray source was operated at 40 kV and 50 mA using a 200 μm focal cup with a graphite monochromator. Data were recorded by collecting a series of oscillation frames, each frame subtending 10′ of arc for a period of 400 s. A total of 300 frames were collected at three different Φ values where the crystals were mounted about the [001] axis. Additional data were collected with the Ω coincident with the [100] direction. Several crystals were required to sample all of reciprocal space.

The four crystallized inhibitor complexes were isomorphous, yet the resolution for the diffraction varied considerable (Table I). The best crystals contained the Phe-Gly isostere (compound Va), and useful data were measured with d spacings greater than 2.5 Å. The diffraction of the Phe-NorVal isostere (compound Vc) fell off quickly after 3.0 Å. The crystals of these four complexes appeared to be isomorphous with those reported by Erickson et al. (1990) for the complex of HIV protease with the inhibitor A-74704. As discussed by Erickson et al. (1990), their crystals exhibited strong noncrystallographic 2-fold symmetry, and they could not unambiguously distinguish between $P6_122$ and $P6_1$ symmetry from the intensity data. We had similar concerns about the classification of our crystals since the diffraction pattern clearly showed $P6/mmm$ symmetry. To explore further the symmetry of the diffraction, the three-dimensional data were processed and reduced to the unique asymmetric unit assuming $P6_1$ and $P6_122$ for purposes of calculating the residual of merged reflections. The R-sym for equivalent reflections due to the 22 symmetry was indistinguishable from the R-sym derived from merging other symmetry-related reflections. While the space group for our crystals appeared to be $P6_122$, the lower symmetry space group could not be ruled out. In the higher symmetry space group the asymmetric unit contains a monomer of the enzyme such that the two halves of the dimer are related by crystallographic symmetry, and the inhibitor is necessarily disordered. The asymmetric unit of the lower symmetry space group contains the dimeric enzyme, and the inhibitor need not be disordered. In general, the classification of the space group is independent of the unit cell contents, and one would follow conventional procedures and choose the higher symmetry space group $P6_122$. However, since there remained some ambiguity and to be consistent with previously reported structures (Erickson et al., 1990), we proceeded to treat the additional symmetry as noncrystallographic and assign the space group as $P6_1$.

Structure Determination. The crystal structures of the four protease–inhibitor complexes were solved by molecular replacement methods. Sets of structure amplitudes were calculated using the coordinates of HIV-1 protease in both the native conformation (Wlodawer et al., 1989) and the conformation when bound to MVT-101 (Miller et al., 1989). The native data for each of the four complexes were expanded to P_1, and 1500 of the strongest intensities were used to calculate the fast rotation function using the structure of the dimer. A single peak, corresponding to a set of Eulerian angles, was produced with both models that was significantly above the background level (4.8 σ and 5.6 σ). Applying the rotation to the preliminary models placed the molecular 2-fold axis

parallel with the [010] crystallographic 2-fold axis, as anticipated from the diffraction symmetry. Using a Fourier-based translation function, we were able to determine the correct enantiomorph and the position of the molecule. Again the largest peak corresponded to a position along the 2-fold axis. Structural amplitudes were calculated from the initial models that resulted in a residual of 42% using data from 10 to 3 Å. The orientation and position of the protein were refined using a rigid-body least squares procedure which reduced the R value to under 38% for all of the complexes. The packing of the molecules in the cell was visually checked using the graphics program DOCK (Stodola et al., 1988). The solution was sterically reasonable and consistent with the pseudo 22 symmetry.

Structure Refinement. The model obtained from the molecular replacement solution for the protein was initially refined with the restrained least squares program PROLSQ (Hendrickson, 1985). Since the two halves of the enzyme are chemically identical, noncrystallographic constraints were imposed on the monomers to maintain identical structures in the initial cycles of refinement. After several cycles of least squares refinement the R value dropped to 32% for data between 10 and 3 Å. Electron density maps were calculated with coefficients $2F_o - F_c$ and $3F_o - 2F_c$ using the model phases. The fit of the model was examined residue by residue, and several torsional angles were adjusted to optimize the fit to the electron density. Data with d spacings >2.5 Å were added, and further cycles of refinement lowered the residual to less than 27%. To further improve the model, omit maps were calculated and the model was readjusted.

The electron density in the vicinity of the inhibitor binding site was diffuse, and the hydroxyethylene isosteres could be built in two orientations that were related by the pseudo-crystallographic 2-fold axis. For example, the Phe-Gly isostere (Va) complex exhibited unambiguous electron density for the benzyl side chain of the isostere in both the S1 and S1′ binding pockets. Models of the inhibitors were built in an extended conformation and positioned in the active site in a fashion similar to that of other published inhibitors (Wlodawer et al., 1989; Fitzgerald et al., 1990; Jaskólski et al., 1991). The least squares program was modified to refine the enzyme and the two copies of the inhibitor simultaneously. Several additional cycles of refinement interspersed with graphical rebuilding reduced the residual further to less than 22%.

The final cycles of refinement were performed using the program XPLOR (Brunger et al., 1987). The noncrystallographic constraints imposed on the dimer were replaced with restraints, and the residual dropped to 19.6%. The restraints were gradually weakened to allow the structure to deviate from 2-fold symmetry. When the restraints were completely removed and the molecules allowed to refine independently for several cycles, the residual dropped further until the final residual for the structures ranged from 18% (for Va) to 16% (for Vb). A summary of crystallographic data for the four complexes is presented in Table I.

Virological Assays

Virus and Cell Lines. The H9 and Molt 4 cell lines have been described (Popovic et al., 1984; Minowada et al., 1972). All cells were maintained in RPMI-1640 containing 10% fetal bovine serum (FBS). H9 cells chronically infected with HIV-1 strain III_B (HIV/III_B cells) (Popovic et al., 1984; Ratner et al., 1985) were established as previously described (Matthews et al., 1987). Briefly, H9 cells were infected with HIV-1 strain III_B at a $TCID_{50}$ to cell number ratio of 1 and grown for a 1–2-week period in RPMI-1640/10% FBS. Cells surviving initial rounds of infection and no longer demonstrating cytopathic effect were grown as chronically infected cells.

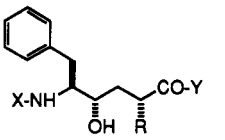

I: X = Boc, Y = Val-NH_2
II: X = Cbz-Ala, Y = Val-NH_2
III: X = Cbz-Ala, Y = Val-Val-OMe
IV: X = Cbz-Ala-Ala, Y = Val-Val-OMe
V: X = Ala-Ala, Y = Val-Val-OMe

FIGURE 1: Structures of inhibitors shown in Tables II and III and Figures 4–7, where R is (a) hydrogen, (b) methyl, (c) *n*-propyl, (d) isobutyl, or (e) benzyl.

SDS–PAGE and Western Blot Analysis. Inhibitors were dissolved in DMSO at 100× concentration and then diluted directly into cultures of chronically infected H9/III_B cells maintained at 37 °C. After 24 h cells were harvested by centrifugation at 1000g for 10 min. Cell pellets were lysed in gel sample buffer and analyzed by SDS–polyacrylamide gel electrophoresis (SDS–PAGE) (Laemmli, 1970). Viral proteins were separated in 12.5% polyacrylamide gels at 40 mA/gel for 4 h and electroblotted onto nitrocellulose filters (Towbin et al., 1979). Western blot detection of p24 and p17 *gag* proteins with mouse monoclonal antibodies (Beckman) was carried out using the Enhanced Chemiluminescence detection system of Amersham.

Acute Infectivity Assays. Molt 4 cells were infected with HIV-1 strain III_B (200 $TCID_{50}$ per 3×10^5 cells), and virus was allowed to adsorb for 1 h at 37 °C. Infected cells were washed by centrifugation at 1500 rpm, resuspended to 3×10^5 cells/mL in fresh RPMI-1640/10% FBS, and transferred to a 24-well assay plate (100 μL in each well). In one protocol, protease inhibitors (10 mM in DMSO) were diluted to 100× their final concentration into medium and then added to the assay wells so that initial calculated inhibitor concentrations ranged from 20 to 0.04 μM in steps of 2-fold dilution. Fresh medium (0.5 mL) was added at 2 and 5 days postinfection, resulting in a final 10-fold dilution of the inhibitor. In a second protocol, the inhibitor concentration was kept constant throughout the 7-day infection cycle as follows: Stock solutions of inhibitor in DMSO were diluted 100-fold directly into assay wells containing acutely infected Molt 4 cell cultures to give final concentrations of 5 μM–1.2 nM inhibitor in steps of 4-fold dilution. At 2 and 5 days postinfection, cultures were fed with fresh medium (0.5 mL) containing inhibitor and 1% DMSO such that the inhibitor concentration was unchanged. For both protocols, after 7 days reverse transcriptase (RT) activity in the medium was measured by quantitation of [^{32}P]TTP incorporation into template DNA (Goff et al., 1981; Willey et al., 1988). Inhibitor treatments were conducted in triplicate and RT assays in duplicate, and the results were averaged. IC_{50} values (the initial concentration of inhibitor required for a 50% reduction of RT activity relative to the value obtained at the highest dilution of inhibitor) were calculated by the method of Karber (1931).

RESULTS

Inhibitor Synthesis. The inhibitors examined in this study incorporate hydroxyethylene isostere analogues of Phe-Gly, Phe-Ala, Phe-NorVal, Phe-Leu, and Phe-Phe (Figure 1).

Scheme I[a]

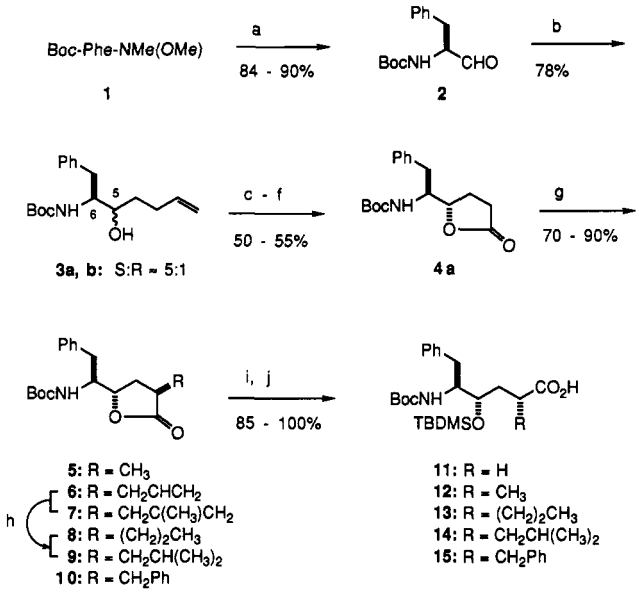

[a] Reagents: (a) $LiAlH_4$; (b) $BrMg(CH_2)_2CHCH_2$, ether/toluene; (c) Ac_2O, Et_3N, 4-(dimethylamino)pyridine; (d) $KMnO_4$; (e) MeONa, MeOH; (f) 10-camphorsulfonic acid, CH_2Cl_2; (g) lithium diisopropylamide, THF, −78 °C, hexamethylphosphoric triamide, RX; (h) H_2, Pd/C, ethyl acetate; (i) NaOH, H_2O/dioxane, citric acid/H_2O; (j) TBDMSCl, imidazole, dimethylformamide; AcOH, H_2O.

Although numerous synthetic routes to hydroxyethylene dipeptide isosteres have been reported (Evans et al., 1985; Fray et al., 1986; Holladay et al., 1987; DeCamp et al., 1991, and references therein), many of these procedures were impractical for the problem at hand or were incompletely described. The synthesis developed for the isosteres of this study (Scheme I) is practical for small- to moderate-scale preparations (1–100-mmol range). In this scheme, the chirality of phenylalanine is used to induce the two new stereogenic centers (C^2, C^4) of the isostere: the C^2 side chain is introduced by alkylation of lactone **4a** (Fray et al., 1986), while chelation-controlled addition of butenylmagnesium bromide to Boc-phenylalanal (**2**) sets the C^4 hydroxyl configuration (Holladay et al., 1987; Jurczak & Golebiowski, 1989).

Lithium aluminum hydride reduction of the *N*-methoxy-*N*-methylamide **1** (Goel et al., 1988; Fehrentz & Castro, 1983) afforded optically pure Boc-phenylalanal (**2**) as a stable solid that showed no tendency to racemize when stored at −20 °C. This preparation of **2** was more convenient and reliable than alternatives such as Swern oxidation of Boc-phenylalanol. The reaction of aldehyde **2** with butenylmagnesium bromide (Holladay et al., 1987) proceeded poorly in tetrahydrofuran, providing an impure product in moderate yield. Best results were obtained by addition of ethereal butenylmagnesium bromide to a solution of aldehyde **2** in toluene at 0 °C to provide the (5*S*)- and (5*R*)-pentenyl alcohols **3a** and **3b** in a ratio of 4–5:1. This reaction invariably returned 15%–20% of the unreacted aldehyde **2**, presumably due to enolization. Addition of $NaBH_4$ to the crude reaction product converted the remaining aldehyde to Boc-phenylalanol, facilitating chromatographic purification of the alcohols **3a,b**. While complete separation of the hydroxy epimers was most conveniently carried out at the lactone stage (i.e., **4a,b**), the ratio of **3a** to **3b** could be readily enhanced to 95:5 by precipitation of the minor isomer from hexane/ethyl acetate. Chiral HPLC analysis of pure **3a** and its enantiomer, synthesized independently from D-phenylalanine, verified that <1% racemization had occurred throughout this sequence (data not shown). Finally, the relative configurations of carbons 5 and 6 in **3a** and **3b** were established from nuclear Overhauser effect (NOE) studies on the oxazolidinones **20a** and **20b** derived from **3a** and **3b**, respectively (Figure 2). Thus, irradiation of the protons H^6 caused strong enhancement of the resonance for H^4 in isomer **20a** but not in isomer **20b**.

The mixture of hydroxy olefins **3a,b** was converted to the lactone **4** through a sequence involving protection of the hydroxyl group, permanganate oxidation of the olefin, hydroxyl deprotection, and lactonization. Chromatography provided pure lactone **4a**, which served as a key intermediate for introduction of a variety of alkyl groups. Initially, alkylation of the dianion of lactone **4a** with methyl iodide under the conditions of Fray et al. (1986) led to lactone **5** in variable yields, along with significant amounts of the dialkylated product. With benzyl bromide, low yields of the desired lactone **10** were obtained. We found that conducting the alkylation reactions at −78 °C in the presence of 2 equiv of hexamethylphosphoric triamide results in reproducible yields of 70%–90% with a variety of alkylating agents including methyl iodide, allyl bromide, methallyl bromide, and benzyl bromide, with little or no dialkylation and nearly complete diastereoselectivity. A strong NOE observed from the C^3 methyl substituent to H^5 in lactone **5** verified that alkylation occurred from the less-hindered face of the lactone enolate to generate the (*R*) configuration at C^2 (Figure 2).

Conversion of the lactones **4a**, **5**, and **8–10** to the protected hydroxyethylene isostere intermediates **11–15** was carried out as described by Evans et al. (1985). These intermediates were employed in standard solution-phase peptide synthesis procedures (Meienhoffer, 1979; Evans et al., 1985) to prepare the array of compounds shown in Figure 1. As illustrated in Scheme II for the synthesis of compound IVb, the mixed anhydride method of peptide coupling was generally used, although in some instances (especially with the bulkier Phe-Phe isostere **15**) higher yields were obtained by use of dicyclohexylcarbodiimide/hydroxybenzotriazole or BOP (Fehrentz & Castro, 1983). A useful property of the TBDMS protecting group concerns the conditions for its removal. As shown in Scheme II, brief treatment of compound **16** with neat trifluoroacetic acid effected removal of the Boc protecting group in the presence of the TBDMS group, which is evidently inductively stabilized by the resulting adjacent ammonium substituent. Removal of the silyl protecting group from the fully blocked peptide **19** was accomplished by treatment with either tetrabutylammonium fluoride or trifluoroacetic acid, although in some cases the latter procedure afforded lower yields due to lactonization of the isostere and ejection of the carboxy-terminal amino acid residues.

Enzyme Inhibition. We previously showed that several peptide mimetics containing the hydroxyethylene isostere analogue of Phe-Gly, including compounds IIIa, IVa, and Va (Table II), are potent linear-competitive inhibitors of HIV-1 protease and that the (*S*) configuration for the hydroxyl group within the isostere (derived from compound **3a**) is essential to potent inhibition (Dreyer, 1989; Meek et al., 1990). To further define the requirements for potent inhibition, we studied the effects of substitution at the P1′ position of the isostere [notation of Schechter and Berger (1967)] as well as variation in the number of flanking residues. Inhibitors were initially evaluated by the method of Dixon (1953). For tight-binding inhibitors ($K_i \leq 20$ nM), inhibition constants were more accurately determined from plots of remaining enzyme activity versus variable inhibitor concentration at several fixed enzyme concentrations. These plots were fitted to eq 1, which takes into account the mutual depletion of free enzyme and

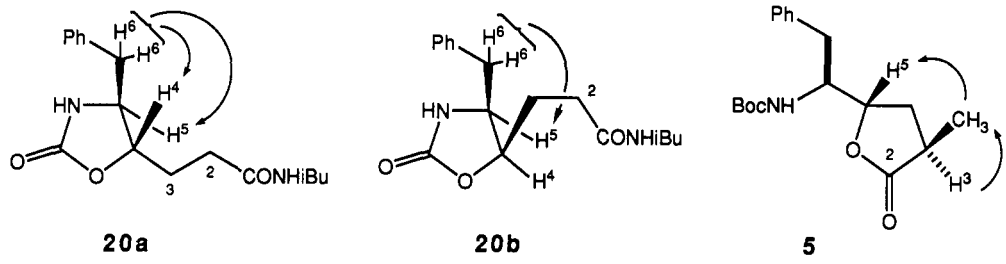

FIGURE 2: Proof of stereochemistry. Observed NOE enhancements are indicated by arrows. Oxazolidinones **20a** and **20b** were synthesized from compounds **11** and **21**, respectively, by the following sequence: (a) *i*-BuOCOCl, *N*-methylmorpholine, *i*-$BuNH_2$; (b) $(n\text{-}Bu)_4NF$; (c) CF_3CO_2H, HCl; (d) $COCl_2$, *n*-methylmorpholine, THF.

Scheme II[a]

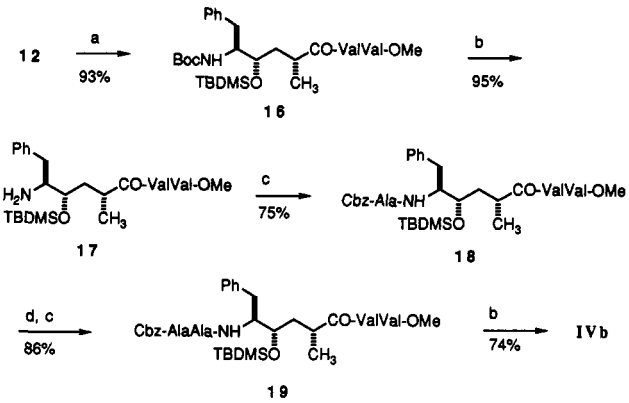

[a] Reagents: (a) *i*-BuOCOCl, *N*-methylmorpholine, THF, –40 °C; HCl·ValVal-OMe, *N*-methylmorpholine; (b) CF_3CO_2H; $NaHCO_3/H_2O$; (c) Cbz-Ala, *i*-BuOCOCl, *N*-methylmorpholine, THF, –40 → 25 °C; (d) H_2, Pd/C, MeOH.

inhibitor as a result of their tight complexation (Williams & Morrison, 1979; Cha, 1975).

Two interdependent factors contribute to inhibition within the series of compounds shown in Table II. Most notably, for compounds with the same peptide length (columns I–IV), inhibition depends on the nature of the substituent, R, within the hydroxyethylene isostere. The values of K_i decrease by factors of 25–73 upon addition of a single methyl group to the P1′ position of the isostere (R = Me vs H). For compounds in columns I and II further increases in the size of R to *n*-propyl, isobutyl, and benzyl lead to successive decreases in K_i by factors of about 3–5, 2–5, and 7–14, respectively. Secondly, for compounds containing the same hydroxyethylene isostere, inhibition depends on inhibitor length and enzyme subsite occupancy. Among the compounds in rows a–c, the largest increases in potency (21–33-fold) correspond to addition of the P3′ valine residue (IIa–c vs IIIa–c). Similar successive increases in potency by factors of 2–6 and 1–3, respectively, occur upon addition of the P2 alanine (Ia–e vs IIa–e) and P3 alanine (IIIa–e vs IVa–e) residues, respectively. Thus residues on the carboxy-terminal (P′) side of the scissile bond appear to contribute more to potency than residues on the amino-terminal (P) side within this series. Compounds lacking a P2′ residue are much weaker, such as BocNHCHBnCH(OH)CH-$BnCONH_2$ for which K_i = 3200 nM.

The contributions to potency afforded by the two factors, inhibitor length and P1′ substituent, are uniform and cumulative so that high K_i values cluster in the upper-left quadrant of Table II and low K_i values occupy the lower-right quadrant. Finally, the inhibition constants for this series converge to about 0.4 nM. As a result of this convergence, the K_i values of compounds within the low-potency region (upper left) of Table II are more sensitive to changes in R or inhibitor length than are those of compounds in the high-potency region (lower right). This "dampening" effect is particularly evident with compounds in row e, which show only small variations in K_i. This may indicate the approach to an optimum binding mode for this series (and may, in addition, reflect a limitation of the present kinetic assay for very tight-binding inhibitors).

Several inhibitors were studied for possible slow-binding behavior by preincubation with HIV-1 protease prior to addition of substrate and analysis of reaction products (Morrison & Walsh, 1988). None of these inhibitors exhibited evidence of a time-dependent increase in inhibitory potency (Table II). In addition, two of the most potent inhibitors, IVd and IVe, failed to exhibit slow-binding behavior when examined in a continuous spectrophotometric assay for HIV-1 protease (Tomaszek et al., 1990; T. Angeles, unpublished data). These results are somewhat surprising in view of the slow-binding inhibition reported for similar inhibitors of porcine pepsin (Holladay et al., 1987).

Three-Dimensional Structure. To better understand the structural basis for inhibition, the crystal structures of four hydroxyethylene isostere inhibitors complexed to HIV-1 protease were determined. The four inhibitors used were compounds Va, Vb, Vc, and Ve (Figure 1), which exhibited K_i values in the peptidolytic assay of 4.0, 3.0, 1.2, and 0.6 nM, respectively. All four complexes crystallized as $P6_1$ hexagonal rods with pseudo 22 symmetry where the two halves of the dimer are related by a pseudo 2-fold axis. The inhibitors lie across (approximately normal to) the 2-fold axis and are disordered with equal populations of inhibitor in each of two orientations. In contrast, Jaskólski et al. (1991) reported that a complex of a hydroxyethylene isostere inhibitor with a synthetic form of HIV protease crystallized in space group $P2_12_12_1$, the asymmetric unit containing the protease dimer and the inhibitor lying mainly if not entirely in one orientation. Despite these differences, the enzyme structure and overall conformation and binding mode of our four inhibitors are similar to those of previously reported HIV protease–inhibitor complexes (Miller et al., 1989; Swain et al., 1990; Fitzgerald et al., 1990; Erickson et al., 1990; Jaskólski et al., 1991). The structure of the protease complexed with these four isosteres is remarkably similar to that described by Erickson et al. (1990) for the complex with the inhibitor A-74704. The overall rms difference of the protein structures for the A-74704 complex and the Phe-Gly isostere (Va) complex is less than 0.55 Å.

In several of the reported HIV protease–inhibitor structures, the inhibitor causes a significant asymmetry in the protein. In the A-74704 complex, a superposition of the two monomers reveals an overall rms deviation of 0.78 Å between the two subunits, the single largest difference being associated with the side chain of Phe53. In our hydroxyethylene isostere complexes the extent of asymmetry is small, with an overall rms deviation of 0.25 Å between the two monomers. To further explore the extent of asymmetry in the complexes, we examined

Table II: Inhibition of HIV-1 Protease by Hydroxyethylene Isosteres[a]

	inhibition constant (K_i, nM)			
inhibitor	I	II	III	IV
a (R = H)	6500 ± 700[b]	2500 ± 180[b]	118 ± 4[b]	44 ± 2[b]
b (R = Me)	260 ± 28[b]	50 ± 8[b]	1.6 ± 0.2	0.6 ± 0.1[c]
c (R = *n*-Pr)	50 ± 4[b]	20 ± 4[c]	0.6 ± 0.2	0.4 ± 0.2
d (R = *i*-Bu)	23 ± 2	3.9 ± 0.4	0.9 ± 0.2	0.8 ± 0.2[c]
e (R = Bn)	1.4 ± 0.2[c]	0.6 ± 0.2	0.6 ± 0.1[c]	0.4 ± 0.1[c]

[a] Except where noted by footnote *b*, inhibition constants were determined by fitting plots of v_i/v_0 vs I_t to eq 1 as described under Materials and Methods. An average of the values for A determined from eq 1 was 1.0 ± 0.2, indicating that the purified HIV-1 protease used was completely active. [b] Inhibition constants determined by Dixon analysis. [c] Examined for time-dependent inhibition by preincubation studies. No time dependence was observed.

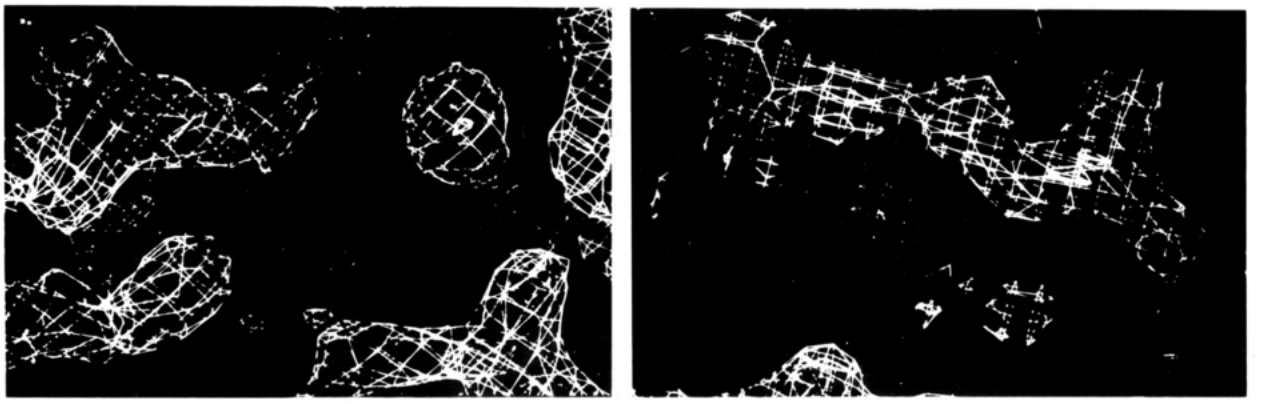

FIGURE 3: Electron density map of the flap region in the HIV-1 protease complex with Va, contoured at 1.5 σ. Disorder of residues Phe53 and Phe53′ is apparent from the low electron density for the benzyl side chain in each monomer (lower center of each panel).

the packing of the protease dimer in the unit cell with respect to lattice contacts. Gln2, Arg14, Glu21, Asn37, Lys41, Gln61, and Lys70 are some of the residues that appear to make strong lattice contacts in both the A-74704 complex and our structures. If the complex were 2-fold symmetric, then rotating the dimer about the 2-fold axis and placing it in the $P6_1$ cell should produce lattice contacts that are indistinguishable from the observed structure. For both the Phe-Gly isostere and A-74704 complexes the same strong lattice contacts are maintained in both orientations, except that, in the A-74704 complex, Phe53 collides with its symmetry-related residue when the dimer is rotated in the lattice. This would consequently break the 22 symmetry, in agreement with the observed space group $P6_1$ for the complex (Erickson et al., 1990). In the structures of our four isostere complexes the electron density for Phe53 is disordered in both monomers as seen in Figure 3. Thus Phe53 is not a useful marker for 22 symmetry in these isostere structures. The lack of obvious differences in lattice contacts for the two subunits further points out the strong pseudo 22 symmetry of these isostere complexes.

In the structures described by Fitzgerald et al. (1990) and Jaskólski et al. (1991), the asymmetry in the "flap" region allows the carbonyl of Ile50′ to accept a hydrogen bond from the amide of Gly51. The complexes with Va–c and Ve are more similar to the structure described by Erickson et al. (1990) in that the tips of the flaps are in van der Waals contact but do not form a hydrogen bond. Fitzgerald et al. (1990) also showed that residues Asn98 and Asn98′ have different conformations and form hydrogen bonds with one another. In our structures these residues are not involved in interactions across the dimer interface. We conclude that the protein structures in the complexes with Va–c and Ve all possess approximate C_2 symmetry and are essentially similar to one another with only slight differences. In a comparison of any two of these complexes the root mean square difference of the C_α coordinates of the proteins is less than 0.6 Å.

The four inhibitors, shown in Figure 4, bind in an extended

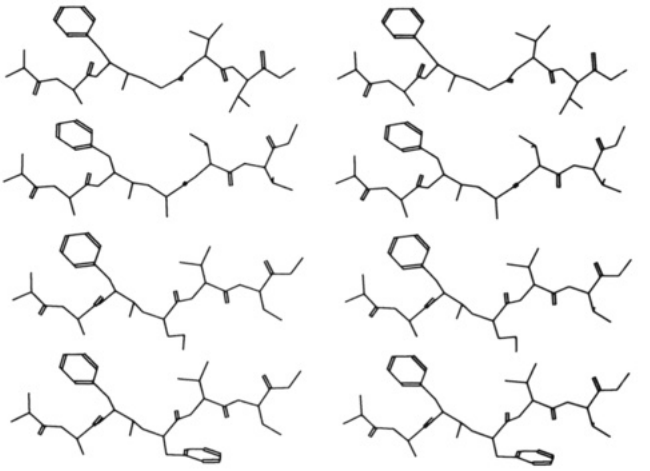

FIGURE 4: Stereoview of inhibitors Va–c and Ve in their bound conformations within the active site of HIV-1 protease.

conformation, making conserved hydrogen bonds and hydrophobic contacts with the enzyme. Potential hydrogen bonds are illustrated in detail for the Phe-Gly isostere (Va) in Figure 5. The (*S*)-hydroxyl group of the isostere lies very close to the enzyme 2-fold axis within H-bonding distance of the catalytic carboxyl groups of Asp25 and Asp25′. The H-bonding network linking enzyme and inhibitor is roughly symmetric with respect to the central hydroxyl group with similar interactions between the two halves of the inhibitor and the two subunits of the enzyme. The approximate symmetry of donor and acceptor interactions is readily apparent from an overlay of the two observed inhibitor orientations, shown in Figure 6 for the Phe-Phe inhibitor Ve. However, as might be expected for an asymmetric inhibitor, the two orientations are offset relative to one another in order to optimize interactions with the enzyme and to preserve the position of the hydroxyl group of the isostere. The carbonyl groups of Gly27 and Gly27′, rotated 90° relative to their positions in the unliganded protease (Navia et al., 1989;

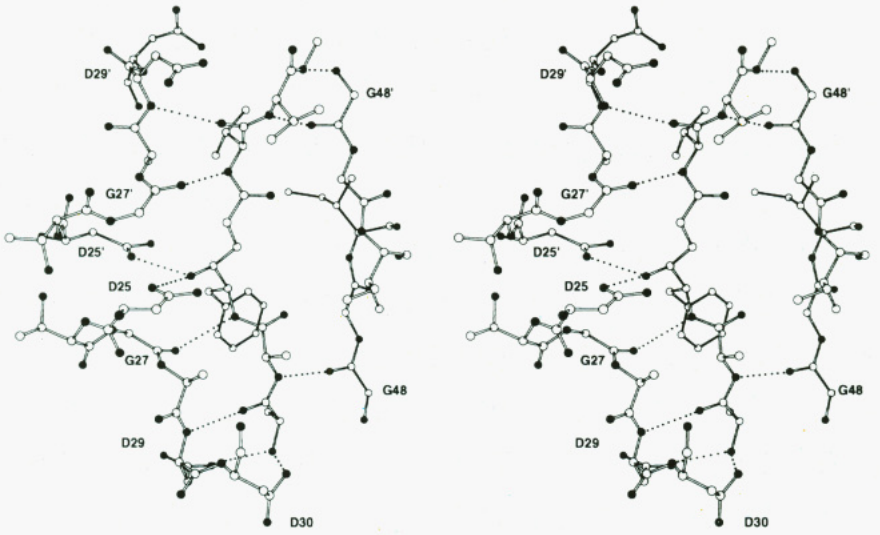

FIGURE 5: Structure of the Phe-Gly isostere (compound Va) bound in the active site of HIV-1 protease. Amino acid residues of the enzyme active site that establish hydrogen bonds with the inhibitor are indicated by their one-letter code designations. Hydrogen bonds are indicated by dotted lines.

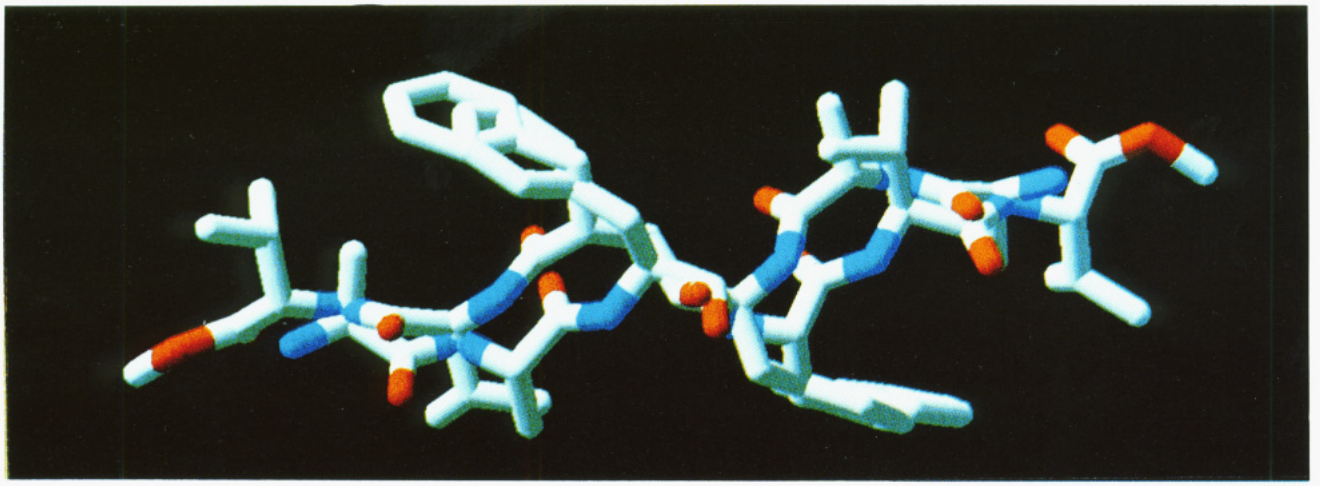

FIGURE 6: Overlay of the two observed orientations of the Phe-Phe isostere (compound Ve) in its bound conformation. The enzyme–inhibitor complex contains equal populations of the inhibitor in each orientation. Carbon is white, nitrogen is blue, and oxygen is red.

Wlodawer et al., 1989; Lapatto et al., 1989), accept H-bonds from the NH groups at P1 and P2′ of the inhibitor, respectively (Figure 5). The carbonyl groups at the inhibitor P2 and P1′ positions point inward, converging to a point corresponding to the position of a conserved water molecule described in other structures (Jaskólski et al., 1991, and references therein). While water molecules were not included in the refinement, weak density is observed in difference Fouriers for a potential water molecule to serve as a bridge from the inhibitor to the NH groups of Ile50 and Ile50′ in the flap region of the enzyme. Difference electron density in the vicinity of the water molecule is weak and diffuse, making it difficult to position the water. H-bonds link the P3 and P2′ carbonyl oxygens with NH of Asp29 and Asp29′ and the P2 and P3′ NH groups with the carbonyls of Gly48 and Gly48′, respectively. At the carboxyl end of the inhibitors, the ester oxygen appears to accept an H-bond from the NH of Gly48′, while the ester methyl group protrudes out of the enzyme and is exposed to solvent. The amino terminus of each inhibitor is unprotected and can ion pair or H-bond with the β-carboxyl group of Asp29 and perhaps that of Asp30. This interaction may account for the increase potency of compound Va (by a factor of 12) relative to its protected counterpart, IVa.

The conformations of the amino-terminal (P) halves of the four inhibitors match closely, while there are significant differences in the carboxy-terminal halves (Figures 4 and 7). As seen from the overlay of the three inhibitors in Figure 7, the greatest conformational differences are in the carboxy terminus of the Phe-Gly isostere. In the Phe-Phe isostere, the P1′ benzyl group fits snugly into a binding pocket (S1′) defined on one side by the side chains of Leu23, Pro81-Val82, and Ile84 from one dimer subunit and bounded on the other side by Ile50′ from the flap of the second subunit. An identical symmetry-related binding pocket houses the P1 benzyl side chain in each of the inhibitors. The binding site for the P2′ valine side chain in the inhibitors, S2′, is a deep pocket bounded on three sides by hydrophobic side chains from Ile47, Val32, Ile84, and Ile50′ and enclosed by the segment Ala28-Asp29 from the active site loop. The corresponding S2 pocket is occupied by the smaller alanine side chain at P2 of the inhibitor. From the overlay in Figure 6 the amino-terminal half of the inhibitor backbone appears distorted, burying the alanine methyl group more deeply in the S2 pocket where it can match the placement of the P2′ valine side chain. This is a common feature of all four structures and suggests that the S2 pocket is not fully utilized by alanine. There is not a well-defined

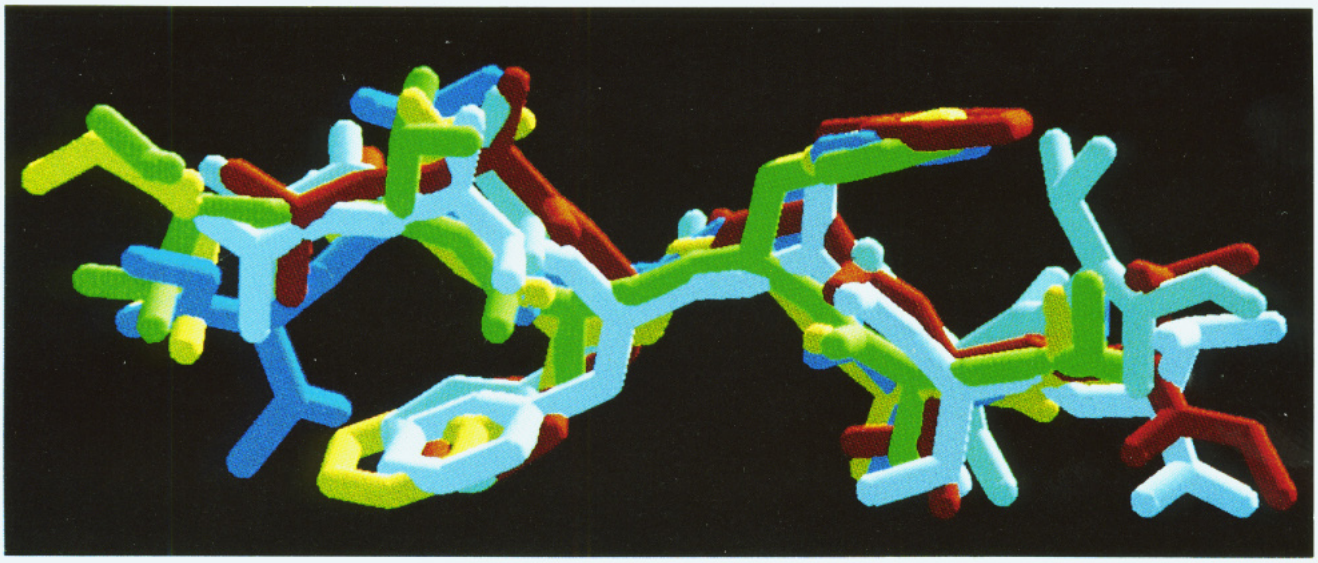

FIGURE 7: Composite view of the bound conformations of three hydroxyethylene isosteres (compounds Va, Vb, Ve), each shown in their two orientations within HIV-1 protease. Each orientation of each inhibitor is colored separately. Compound Va is shown in light blue and dark blue, Vb in white and green, and Ve in red and yellow. (Compound Vc was omitted for clarity.)

pocket corresponding to S3′ (or S3), and in fact the P3′ valine side chain in the Phe-Ala, Phe-NorVal, and Phe-Phe inhibitors is substantially exposed to exterior solvent. The backbone of the Phe-Gly inhibitor Va, however, curls back to partially bury the P3′ valine side chain in the S1′ pocket (Figure 7), perhaps compensating for the lack of a P1′ side chain in the Phe-Gly isostere. In Vb, Vc, and Ve, while the peptide backbone is fully extended, the P1′ and P3′ side chains are in van der Waals contact and effectively fill the extended S1′/S3′ pocket. Similarly, in all four inhibitors the P1 and P3 side chains are in contact within the S1/S3 pocket.

Cell Culture Assays. We showed previously that compounds IIIa and IVa, when added at a dose of 25 μM to chronically infected T-cells, inhibit HIV-1 protease within the context of steady-state virus production (Meek et al., 1990). A hallmark of protease inhibition within these cells is the accumulation of the Pr55 precursor and three partially processed forms with apparent molecular masses of 25, 40, and 47 kDa (most likely representing p24–p1, a mixture of p17–p24–p1 and p24–p1–p7–p6, and p17–p24–p1–p7, respectively) and a corresponding decrease in the levels of mature p17 and p24. In addition, compounds IIIa and IVa are protective in acute infectivity assays with a freshly infected T-cell line (Meek et al., 1990). For the present study, we examined a selection of compounds from Table II in order to correlate their K_i values with their activities in chronically and acutely infected cells.

Human H9 T-cells chronically infected with HIV-1 strain III_B (Popovic et al., 1984) were treated for 24 h with compounds IIa–e, IIIe, and IVe at concentrations ranging from 10 to 0.078 μM in steps of 2-fold dilution. Western blots of electrophoretically separated proteins from cell lysates were probed with p17- and p24-specific monoclonal antibodies (Figure 8). Samples from cultures treated with any concentration of compound IIa appear identical to untreated controls, exhibiting substantial amounts of p17 and p24 relative to Pr55 and no intermediates (Figure 8A). In contrast, compounds IIb–e, IIIe, and IVe produced dose-dependent increases in the levels of p40, p47, and Pr55 and decreases in p17 and p24 relative to Pr55 (Figure 8B–G). With increasing inhibitor concentration the first intermediate to appear is p40, followed by p47. This order of appearance of p40 and p47 is consistent with studies of the in vitro processing of recombinant Pr55 (Erickson-Viitanen et al., 1989) and of model peptide substrates (Darke et al., 1989; Moore et al., 1989), suggesting that the kinetic efficiency (V/K) of the p1–p7 cleavage junction (Met377-Met378 of Pr55) within the p47 protein is greater than that of the p17–p24 cleavage junction (Tyr132-Pro133 of Pr55). At the higher concentrations of the more potent inhibitors the formation of the p40 and p47 intermediates is also inhibited so that almost all of the detectable protein appears in the $Pr55^{gag}$ band (Figure 8E–G). We have defined the minimum inhibitory concentration (MIC) in the Western blot assay as the lowest concentration of inhibitor at which processing intermediates, especially p40, are observed. By this definition, the MIC values range from 10 μM for compound IIb to about 0.3 μM for compound IVe and show a rank-order correlation with the values of K_i for these compounds (Table III). However, the MIC values are greater than corresponding K_i values by factors of about 100–1000.

To assess antiinfective potency in an acute infection assay, protease inhibitors were added to cultures of Molt 4 cells 1 h following infection with HIV-1. The cultures were maintained for 7 days with periodic additions of fresh medium, after which the RT in culture supernatants was measured. As summarized in Table III, the IC_{50} values in this assay, defined as the *initial* inhibitor concentration required for a 50% reduction in RT activity relative to control, are similar to the MIC values in chronic infection and are approximately correlated with inhibitor K_i values. Compound IIa is not antiviral at concentrations up to 20 μM, while IC_{50} values for the more potent inhibitors fall in the range 0.1–1 μM. Nevertheless, we were concerned that the potency of the inhibitor may be compromised under the conditions of this assay, since the inhibitor is added only at the time of infection and is diluted with medium to 10% of its initial value in the course of the assay. Although this protocol entails the least possible manipulation of the system, the resulting dilution of the inhibitor leads to ambiguity in the calculated IC_{50} values. In addition, potential compound instability or insolubility over the 7-day assay period could further reduce activity. The

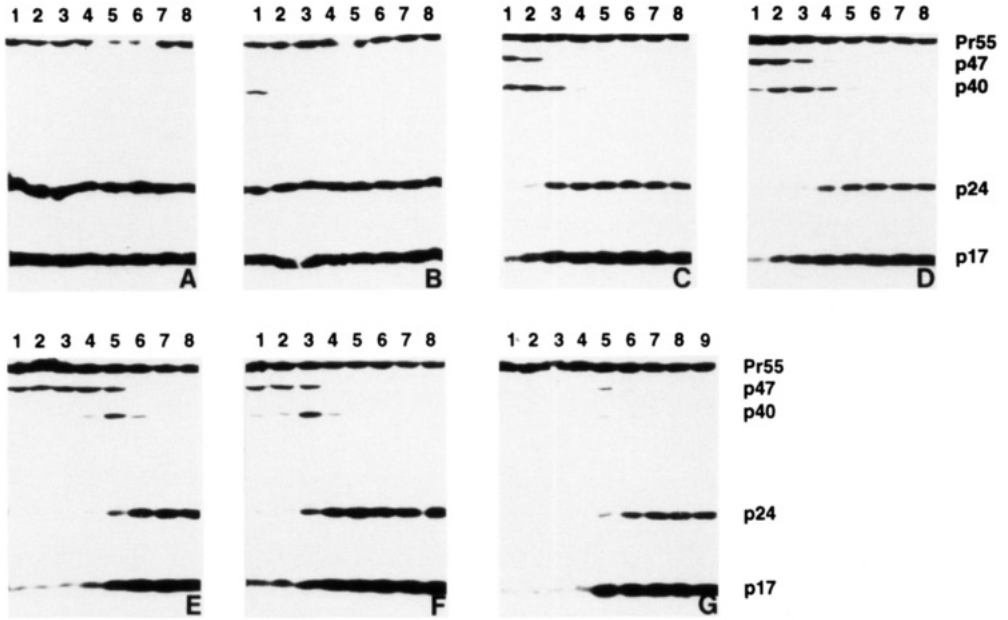

FIGURE 8: Western blot analysis of Pr55^{gag} processing inhibition in chronically infected T-cells. H9 cells chronically infected with HIV-1 were cultured in the presence of protease inhibitors for 24 h as described under Materials and Methods. Cell pellets were disrupted in SDS and analyzed by SDS–PAGE. Detection of viral proteins within the electroblots utilized p24 and p17 mouse monoclonal antibodies and horseradish peroxidase-conjugated goat anti-mouse IgG. Inhibitors used were compounds IIa (A), IIb (B), IIc (C), IId (D), IIe (E), IIIe (F), and IVe (G). Inhibitor concentrations were 10 μM (lanes 1), 5 μM (lanes 2), 2.5 μM (lanes 3), 1.3 μM (lanes 4), 0.63 μM (lanes 5), 0.31 μM (lanes 6), 0.16 μM (lanes 7), and 0.078 μM (lanes 8). Lane 9 in panel G is a control with no inhibitor.

Table III: Inhibition of Proteolytic Processing in Chronically Infected T-Cells and Inhibition of Infectivity in Acutely Infected T-Cells

inhibitor (K_i, nM)[a]	chronic infection, MIC (μM)[b]	acute infection, IC_{50} (μM)[c]
IIa (2500)	ni	ni
IIb (50)	10	8.0
IIc (20)	2.5	7.6
IId (3.9)	1.2	0.96
IIe (0.6)	0.3	0.85
IIIe (0.6)	0.6	0.52
IVe (0.4)	0.3	0.31
Ie (1.4)	0.6	0.17, 0.028[d]

[a] Values from Table II. [b] Values estimated from Western blots in Figure 8 (data not shown for Ie). MIC = lowest concentration of inhibitor resulting in visible processing inhibition. [c] Fifty percent inhibition (IC_{50}) end points determined by measuring the RT in the culture medium of inhibitor-treated acutely infected Molt 4 cells after 7 days as described under Materials and Methods. Except where noted by footnote *d*, inhibitor was added in a single portion and was diluted 10-fold over the course of the assay (first protocol of Materials and Methods). [d] Value determined as in footnote *c* except that the inhibitor concentration was held constant over the course of the assay (second protocol).

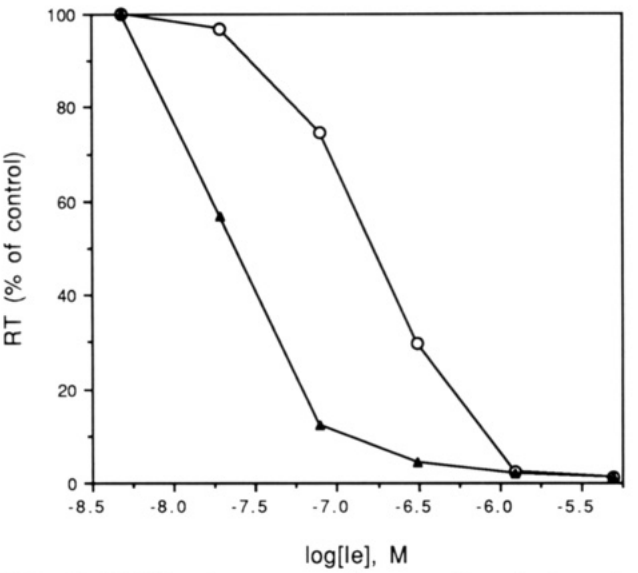

FIGURE 9: Inhibitory dose–response of compound Ie under two acute infectivity assay protocols. Molt 4 cells freshly infected with HIV-1 strain III_B were treated with serial dilutions of compound Ie either in a single portion (first protocol of Materials and Methods) (open circles) or in three portions to maintain constant inhibitor concentrations (second protocol) (triangles). After 7 days RT in culture supernatants was quantified as described under Materials and Methods.

assay was therefore modified to maintain a constant inhibitor concentration. In this second assay protocol, fresh inhibitor was added to the cultures along with medium at two intervals during the assay period. Consistent with our expectations, with this modification the IC_{50} value for compound Ie is 28 nM, 6-fold lower than with the first protocol (Table III, Figure 9).

DISCUSSION

The array of compounds in Table II encompasses stepwise structural changes that, in conjunction with information gained from crystallographic studies, enable us to define the elements necessary for potent inhibition of HIV-1 protease by hydroxyethylene isosteres. The data indicate that minimal structures exhibiting tight-binding ($K_i < 10^{-8}$ M) inhibition are composed of an amino-protected hydroxyethylene isostere joined to a P2′ amino acid amide (Figure 10). Further truncation results in a significant loss in potency. A "core" structure for inhibition therefore consists of four side chains corresponding to substrate residues P2–P2′ and three carboxamide groups including the P2′ carboxamide terminus and the two carboxamide links joining P2–P1 and P1′–P2′. Additional significant but smaller contributions to binding affinity arise from aminoacyl residues in the P3 and P3′ positions.

The compounds in Table II show the importance of the P1′ side chain, which alone is responsible for potency increases of as much as 4600-fold (Ia vs Ie). This highlights the significance of hydrophobic interactions with the S1′ pocket

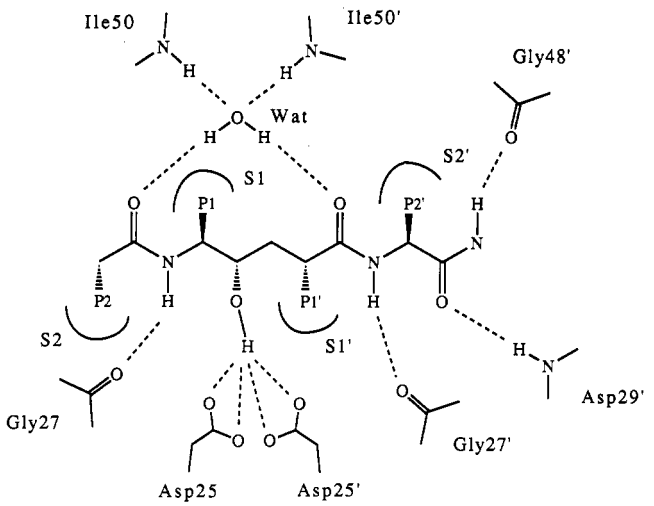

FIGURE 10: Minimum interactions required for tight-binding inhibition of HIV-1 protease by hydroxyethylene isosteres. Seven essential hydrogen bonds to the inhibitor and four binding pockets (S2–S2′) are indicated.

and serves to explain the alterations in the conformation of the Phe-Gly inhibitor Va in which the P3′ valine side chain extends into the S1′ pocket (Figures 5 and 7). A similar phenomenon occurs in a complex of *Rhizopus chinensis* pepsin with its very potent inhibitor, pepstatin A (Bott et al., 1982). Pepstatin A lacks a P1′ side chain, and the side chain of the P3′ residue reaches back to fill the S1′ pocket of pepsin. Curiously, however, no such "illicit occupation" is seen in a complex of pepstatin A with HIV-1 protease (Fitzgerald et al., 1990). This might help to explain our previous observation that HIV-1 protease is inhibited relatively poorly by pepstatin A and analogues but far more effectively by closely analogous inhibitors containing Phe-Gly hydroxyethylene isosteres (Dreyer et al., 1989). Furthermore, the large potency increase resulting upon incorporation of a P3′ residue into the Phe-Gly inhibitors (IIa and IIIa) is easily rationalized by the crystallographic data. In contrast, the Phe-Phe inhibitors, which feature a nearly optimal P1′ side chain, gain little from a P3′ residue (IIe vs IIIe). While these results illustrate that the P1′ side chain is especially important to binding, variation of the equally important side chains P2, P1, and P2′ must also be examined in a thorough optimization study.

Of particular interest are potent inhibitors which do not exactly follow the formula shown in Figure 10 but which apparently achieve equivalent interactions, or find alternative compensating ones, using nonpeptide components. An example is the use of benzocycloalkylamines as replacements for the P2′ residue in hydroxyethylene isostere inhibitors (Lyle et al., 1991). The conservation of H-bonding and hydrophobic interactions within these increasingly nonpeptide inhibitors reinforces the validity of the binding model in Figure 10 and illustrates its value for inhibitor design. It is worth mentioning in this regard that the Boc carbamate group is a special P2 residue, since compounds containing the analogous amide, *tert*-butylacetyl, are 10-fold less potent (Vacca et al., 1991; Dreyer et al., unpublished observations). The origin of the enhanced affinity for carbamate termini is unexplained but might indicate a conformational effect or a specific active site interaction of the urethane oxygen.

The minimal inhibitor model in Figure 10 provides a starting point for inhibitor design in efforts to achieve an acceptable pharmacological profile for in vivo use. Critical to the successful application of these agents is the need to attain sustained antiviral drug concentrations at the relevant sites of infection. These efforts require an understanding of relationships between the enzyme inhibition constant for these compounds and their antiviral activity in appropriate models. Here, antiviral activity has been evaluated in two separate in vitro assays, involving acutely and chronically infected T-cell systems. While not directly related to in vivo infection, these assay systems may be relevant models for two different contributing aspects of HIV infection. The acute infection assay may mirror the rapid replication and cytopathology responsible, at least in part, for loss of T4-lymphocytes in vivo (Schnittman et al., 1989). In addition, both chronically infected (integrated provirus, continuous expression) and latently infected (integrated provirus, no expression) T-lymphocytes have been implicated as reservoirs of infectious virus contributing to disease progression (Hoxie et al., 1985; Fauci, 1988; Poli et al., 1989; Schnittman et al., 1989). Therefore, in developing guidelines to select compounds for in vivo study, it is important to examine their antiviral potency in models of both acute and chronic infection.

The compounds in Table III show an approximate rank-order correspondence between K_i value with HIV-1 protease and IC_{50} in the acute infection assay, but there is a 20–1000-fold difference between these two values. Factors contributing to this disparity might include degradation, inefficient membrane permeability, or poor solubility of these inhibitors. In evidence that membrane association or transport is an important variable, we have found that highly water-soluble peptide analogues are poorly active in cell-based assays regardless of K_i value (Meek et al., 1990; Lambert et al., unpublished results), while more active inhibitors are highly hydrophobic. Paradoxically, the low water solubility of active inhibitors raises the likelihood that their activity in cells is compromised by precipitation or aggregation. As shown with compound Ie (Figure 9), it is possible to narrow the gap between K_i and IC_{50} values with slight changes in assay conditions. By periodic addition of inhibitor over the time course of the assay, the effects of dilution or precipitation of the inhibitor are apparently overcome, leading to a lower IC_{50}. Moreover, a similar enhancement of potency under these modified assay conditions has been observed with other inhibitors. This suggests that the IC_{50} values in Table III are overestimates of the concentrations of these compounds capable of inhibiting acute infection. It is evident that careful manipulation of these structures may be necessary to reach a balance of aqueous solubility and lipophilicity that optimizes their antiviral potential.

In comparison with the potent acute antiinfective activity attainable with protease inhibitors, Western blot analysis suggests that relatively high inhibitor concentrations are required for efficient processing inhibition in chronically infected H9 cells (Figure 8). This raises the possibility that populations of infected cell types could exist in vivo with differing responsiveness to protease inhibitor treatment. One explanation for this difference could be the high constitutive level of virus expression in H9/III_B cells (Popovic et al., 1984). However, comparisons between the results of the acute and chronic infection assays are not easily interpreted since the mechanistic relationship between the antiviral responses observed in chronic and acute infection is not completely understood. We have shown that, in chronically infected T-cells, antiviral effects of protease inhibitor treatment are manifested by the continued production of immature, noninfectious virions (Lambert et al., 1992). Further experiments are needed to define (1) the quantitative relationship between the extent of processing inhibition and the production of

infectious virus and (2) the mechanism of the replication defect associated with processing inhibition. There is also evidence that, in addition to the *gag/gag-pol* processing occurring during virion assembly, replicative steps involving proviral integration (Baboonian et al., 1991) and activation of proviral transcription (Rivière et al., 1991) may require the action of the retroviral protease. These additional mechanisms could lead to acute antiinfective potency of protease inhibitors beyond that which might be expected from the chronically infected T-cell assay.

Data generated by use of synthetic chemistry, enzyme kinetics, and X-ray crystallography reveal the mode of inhibition and the minimal structural requirements for a class of HIV-1 protease inhibitors (hydroxyethylene isosteres). Infected cell culture assays allow determination of both the enzyme binding affinity and physicochemical properties needed for an effective antiviral agent in vitro. As structural and physical properties (e.g., hydrophobicity) optimal for these in vitro assays are not necessarily concordant with the needs of drug formulation and delivery, pharmacokinetic data are essential for guiding further chemical modification. Only by the interdependent application of these various methods can we select from a large array of inhibitors those with the best potential for clinical efficacy.

ACKNOWLEDGMENT

We thank Stephen A. Carr and the Mass Spectrometry Facility in the Physical and Structural Chemistry Department of SmithKline Beecham Pharmaceuticals for mass spectral analyses, Edith A. Reich for elemental analyses, and Karl F. Erhard for chiral HPLC analysis. We also thank Jeffrey Culp for help with purification of HIV-1 protease and John Erickson (NCI-FCRDC, Frederick, MD) for providing the coordinates of the HIV protease–A74704 complex. We are grateful for helpful discussions with Renée DesJarlais concerning the structures of the protease–inhibitor complexes and with Lucinda Ivanoff concerning cell assay conditions.

SUPPLEMENTARY MATERIAL AVAILABLE

Spectral and analytical characterization data for all inhibitors and for compounds **1–21** (7 pages). Ordering information is given on any current masthead page.

REFERENCES

Ashorn, P., McQuade, T. J., Thaisrivongs, S., Tomasselli, A. G., Tarpley, G. W., & Moss, B. (1990) *Proc. Natl. Acad. Sci. U.S.A. 87*, 7472–7476.

Baboonian, C., Dalgleish, A., Bountiff, L., Gross, J., Oroszlan, S., Rickett, G., Smith-Burchnell, C., Troke, P., & Merson, J. (1991) *Biochem. Biophys. Res. Commun. 179*, 17–24.

Brunger, A. T., Kuriyan, J., & Karplus, M. (1987) *Science 235*, 458–460.

Cha, S. (1975) *Biochem. Pharmacol. 24*, 2177–2185.

Darke, P. L., Nutt, R. F., Brady, S. F., Garsky, V. M., Cicarone, T. M., Leu, C.-T., Lumma, P. K., Freidinger, R. M., Veber, D. F., & Sigal, I. S. (1988) *Biochem. Biophys. Res. Commun. 156*, 297–303.

Debouck, C., Gorniak, J. G., Strickler, J. E., Meek, T. D., Metcalf, B. W., & Rosenberg, M. (1987) *Proc. Natl. Acad. Sci. U.S.A. 84*, 8903–8906.

DeCamp, A. E., Kawaguchi, A. T., Volante, R. P., & Shinkai, I. (1991) *Tetrahedron Lett. 16*, 1867–1870.

Dixon, M. (1953) *Biochem. J. 55*, 170–171.

Dreyer, G. B., Metcalf, B. W., Tomaszek, T. A., Carr, T. J., Chandler, A. C., Hyland, L., Fakhoury, S. A., Magaard, V. W., Moore, M. L., Strickler, J. E., Debouck, C., & Meek, T. D. (1989) *Proc. Natl. Acad. Sci. U.S.A. 86*, 9752–9756.

Erickson, J., Neidhart, D. J., VanDrie, J., Kempf, D. J., Wang, X. C., Norbeck, D. W., Plattner, J. J., Rittenhouse, J. W., Turon, M., Wideburg, N., Kohlbrenner, W. E., Simmer, R., Helfrich, R., Paul, D. A., & Knigge, M. (1990) *Science 249*, 527–533.

Erickson-Viitanen, S., Manfredi, J., Viitanen, P., Tribe, D. E., Tritch, R., Hutchinson, C. A., III, Loeb, D. D., & Swanstrom, R. (1989) *Aids Res. Hum. Retroviruses 5*, 577–591.

Evans, B. E., Rittle, K. E., Homnick, C. F., Springer, J. P., Hirshfield, J., & Veber, D. F. (1985) *J. Org. Chem. 50*, 4615–4625.

Fauci, A. S. (1988) *Science 239*, 617–622.

Fehrentz, J.-A., & Castro, B. (1983) *Synthesis*, 676.

Fitzgerald, P. M. D., McKeever, B. M., VanMiddlesworth, J. F., Springer, J. P., Heimbach, J. C., Leu, C.-T., Herber, W. K., Dixon, R. A. F., & Darke, P. L. (1990) *J. Biol. Chem. 265*, 14209–14219.

Fray, A. H., Kaye, R. L., & Kleinman, E. F. (1986) *J. Org. Chem. 51*, 4828–4833.

Goel, O. P., Krolls, U., Stier, M., & Kesten, S. (1988) *Org. Synth. 67*, 69–75.

Goff, S., Traktman, P., & Baltimore, D. (1981) *J. Virol. 38*, 239–248.

Gottlinger, H. G., Sodroski, J. G., & Haseltine, W. A. (1989) *Proc. Natl. Acad. Sci. U.S.A. 86*, 5781–5785.

Grant, S. K., Deckman, I. C., Minnich, M. D., Culp, J., Franklin, S., Dreyer, G. B., Tomaszek, T. A., Jr., Debouck, C., & Meek, T. D. (1991) *Biochemistry 30*, 8424–8434.

Greenlee, W. J. (1990) *Med. Res. Rev. 10*, 173–236.

Hendrickson, W. A. (1985) *Methods Enzymol. 115*, 252–270.

Holladay, M. W., Salituro, F. G., & Rich, D. H. (1987) *J. Med. Chem. 30*, 374–383.

Hoxie, J. A., Haggarty, B. S., Rackowski, J. L., Pillsbury, N., & Levy, J. A. (1985) *Science 229*, 1400–1402.

Humphrey, M. J., & Ringrose, P. S. (1986) *Drug Metab. Rev. 17*, 283–310.

Jaskólski, M., Tomasselli, A. G., Sawyer, T. K., Staples, D. G., Heinrikson, R. L., Schneider, J., Kent, S. B. H., & Wlodawer, A. (1991) *Biochemistry 30*, 1600–1609.

Jurczak, J., & Golebiowski, A. (1989) *Chem. Rev. 89*, 149–164.

Karber, G. (1931) *Arch. Exp. Pathol. Pharmakol. 162*, 480–483.

Kohl, N. E., Emini, A. E., Schleif, W. A., Davis, L. J., Heimbach, J. C., Dixon, R. A. F., Scolnick, E. M., & Sigal, I. S. (1988) *Proc. Natl. Acad. Sci. U.S.A. 85*, 4686–4690.

Kramer, R. A., Schaber, M. D., Skalka, A. M., Ganguly, K., Wong-Staal, F., & Reddy, E. P. (1986) *Science 231*, 1580–1584.

Laemmli, U. K. (1970) *Nature (London) 227*, 680–685.

Lambert, D. M., Petteway, S. R., Jr., McDanal, C. E., Hart, T. K., Leary, J. J., Dreyer, G. B., Meek, T. D., Bugelski, P. J., Bolognesi, D. P., Metcalf, B. W., & Matthews, T. J. (1992) *Antimicrob. Agents Chemother. 36*, 982–988.

Lapatto, R., Blundell, T., Hemmings, A., Overington, J., Wilderspin, A., Wood, S., Hawrylik, S. H., Lee, S. E., Scheld, K. G., & Hobart, P. M. (1989) *Nature (London) 342*, 299–302.

Lyle, T. A., Wiscount, C. M., Guare, J. P., Thompson, W. J., Anderson, P. S., Drake, P. L., Zugay, J. A., Emini, E. A., Schleif, W. A., Quintero, J. C., Dixon, R. A. F., Sigal, I. S., & Huff, J. R. (1991) *J. Med. Chem. 34*, 1228–1230.

Matthews, T. J., Weinhold, K. J., Lyerly, H. K., Langlois, A. J., Wigzell, H., & Bolognesi, D. P. (1987) *Proc. Natl. Acad. Sci. U.S.A. 84*, 5424–5428.

Meek, T. D., Lambert, D. M., Dreyer, G. B., Carr, T. J., Tomaszek, T. A., Moore, M. L., Strickler, J. E., Debouck, C., Hyland, L. J., Matthews, T. J., Metcalf, B. W., & Petteway, S. R. (1990) *Nature (London) 343*, 90–92.

Meienhofer, J. (1979) in *The Peptides* (Gross, E., & Meienhofer, J., Eds.) Vol. 1, pp 263–314, Academic, New York.

Miller, M., Schneider, J., Sathyanarayana, B. K., Toth, M. V., Marshall, G. R., Clawson, L., Selk, L., Kent, S. B. H., & Wlodawer, A. (1989) *Science 246*, 1149–1152.

Minowada, J., Ohnuma, T., & Moore, G. E. (1972) *J. Natl. Cancer Inst. 49*, 891–895.

Moore, M. L., Bryan, W. M., Fakhoury, S. A., Magaard, V. W., Huffman, W. F., Dayton, B. D., Meek, T. D., Hyland, L., Dreyer, G. B., Metcalf, B. W., Strickler, J. E., Gorniak, J. G., & Debouck, C. (1989) *Biochem. Biophys. Res. Commun. 159*, 420–425.

Morrison, J. F., & Walsh, C. T. (1988) *Adv. Enzymol. Relat. Areas Mol. Biol. 61*, 201–301.

Navia, M. A., Fitzgerald, P. M. D., McKeever, B. M., Leu, C.-T., Heimbach, J. C., Herber, W. K., Sigal, I. S., Darke, P. L., & Springer, J. P. (1989) *Nature (London) 337*, 615–620.

Peng, C., Ho, B. K., Chang, T. W., & Chang, N. T. (1989) *Virology 63*, 2550–2556.

Petteway, S. R., Jr., Dreyer, G. B., Meek, T. D., Metcalf, B. W., & Lambert, D. M. (1991) in *Acids Research Reviews* (Koff, W. C., Wong-Staal, F., & Kennedy, R. C., Eds.) Vol. 1, Chapter 15, pp 267–288, Marcel Dekker, New York.

Poli, G., Orenstein, J. M., Kinter, A., Folks, T. M., & Fauci, A. S. (1989) *Science 244*, 575–577.

Ratner, L., Haseltine, W., Pataraca, R., Livak, K. J., Starcich, B., Josephs, S. F., Doran, E. R., Rafalski, J. A., Whitehorn, E. A., Baumeister, K., Ivanoff, L., Petteway, S. R., Jr., Pearson, M. L., Lautenberger, L. A., Papas, T. S., Ghrayeb, J., Chang, N. T., Gallo, R. C., & Wong-Staal, F. (1985) *Nature (London) 313*, 277–284.

Rich, D. H., Green, J., Toth, M. V., Marshall, G. R., & Kent, S. B. H. (1990) *J. Med. Chem. 33*, 1285–1288.

Rivière, Y., Blank, V., Kourilsky, P., & Israel, A. (1991) *Nature (London) 350*, 625–626.

Roberts, N. A., Martin, J. A., Kinchington, D., Broadhurst, A. V., Craig, J. C., Duncan, I. B., Galpin, S. A., Handa, B. K., Kay, J., Krohn, A., Lambert, R. W., Merrett, J. H., Mills, J. S., Parkes, K. E. B., Redshaw, S., Ritchie, A. J., Taylor, D. L., Thomas, G. J., & Machin, P. J. (1990) *Science 248*, 358–361.

Schechter, I., & Berger, A. (1967) *Biochem. Biophys. Res. Commun. 27*, 157–162.

Schnittman, S. M., Psallidopoulos, M. C., Lane, H. C., Thompson, L., Baseler, M., Massari, F., Fox, C. H., Salzman, N. P., & Fauci, A. S. (1989) *Science 245*, 305–308.

Stodola, R. K., Wood, W. D., Manion, F. J., Berman, H. M., & Badler, N. (1988) in *Crystallographic Computing* (Isaacs, N. W., & Taylor, M. R., Eds.) Vol. 4, pp 223–246, Oxford University Press, Oxford.

Strickler, J. E., Gorniak, J., Dayton, B., Meek, T., Moore, M., Magaard, V., Malinowski, J., & Debouck, C. (1989) *Proteins 6*, 139–154.

Swain, A. L., Miller, M., Green, J., Rich, D. H., Schneider, J., Kent, S. B. H., & Wlodawer, A. (1990) *Proc. Natl. Acad. Sci. U.S.A. 87*, 8805–8809.

Tomasselli, A. G., Olsen, M. K., Hui, J. O., Staples, D. J., Sawyer, T. K., Heinrikson, R. L., & Tomich, C.-S. C. (1990) *Biochemistry 29*, 264–269.

Tomaszek, T. A., Jr., Magaard, V. W., Bryan, H. G., Moore, M. L., & Meek, T. D. (1990) *Biochem. Biophys. Res. Commun. 168*, 274–280.

Towbin, H., Staehelin, T., & Gordon, J. (1979) *Proc. Natl. Acad. Sci. U.S.A. 76*, 4350–4354.

Vacca, J. P., Guare, J. P., deSolms, S. J., Sanders, W. M., Giuliani, E. A., Young, S. D., Darke, P. L., Zugay, J., Sigal, I. S., Schleif, W. A., Quintero, J. C., Emini, E. A., Anderson, P. S., & Huff, J. R. (1991) *J. Med. Chem. 34*, 1225–1228.

Veronese, F. D., Rahman, R., Copeland, T. D., Oroszlan, S., Gallo, R. C., & Sarngadharan, M. G. (1987) *Aids Res. Hum. Retroviruses 5*, 253–264.

Willey, R. L., Smith, D. H., Lasky, L. A., Theodore, T. S., Earl, P. L., Moss, B., Capon, D. J., & Martin, M. (1988) *J. Virol. 62*, 139–147.

Williams, J. W., & Morrison, J. F. (1979) *Methods Enzymol. 63*, 437–467.

Wlodawer, A., Miller, M., Jaskólski, M., Sathyanarayana, B. K., Baldwin, E., Weber, I. T., Selk, L. M., Clawson, L., Schneider, J., & Kent, S. B. H. (1989) *Science 245*, 616–621.